HiSST: 4th International Conference on
High-Speed Vehicle Science Technology
22 -26 September 2025, Tours, France

Design and Experimental Characterisation of a 2D Mach 7 Mixed-Compression Intake

Andrew Hyslop[1], Rowland Penty Geraets[1], Sebastien Wylie[1], Jim Merrifield[1] and Matthew McGilvray [2]

Abstract

The operational modes and self-starting characteristics of a sub-scale, Mach 7, 2D mixed-compression intake were experimentally investigated as a function of imposed back-pressure and isolator height. The experiments were conducted in the University of Oxford High Density Tunnel at a freestream unit Reynolds number of 13.6 x 10^6 m^{-1} at a Mach 7 flight representative condition. The self-starting ability of the intake was shown to be highly sensitive to isolator height, with heights below the Kantrowitz limit shown to be not self-starting for this intake configuration. The imposed back-pressure of the intake could be varied by actuating a wedge to change the throttle area at the isolator exit. A sweep of back-pressure was conducted for two isolator heights (5.9 mm and 7 mm). For each sweep, three modes of operation were identified: started, oscillatory isolator, and buzz. At each operational regime, pressure traces along the intake are shown as well as captured mass flow measurements. The experiments successfully showed that an intake behaviour can be characterised with varying back-pressure and this approach can be extended to more complex intakes in the future.

Keywords: *Intake, Scramjet, Hypersonic, Wind Tunnel*

Nomenclature

Latin
A – Area, m^2
h – Height, m
$\dot{m}$ – Mass flow rate, kg/s
P – Static pressure, Pa
R – Gas constant, J/kg.K
T – Static temperature, K

Greek
γ – Ratio of specific heats
Δ – Throttle ratio
Subscripts
cl – cowl
th - throat

1. Introduction

The design of a scramjet intake is a complex process with plenty of competing design criteria. A key criterion is that they remain in a "started" state for the duration of flight so that design conditions are fed to the combustor and thrust is generated. The definition of a started intake is given by Van Wie [1]: "'started' is used to denote operation under conditions where flow phenomena in the internal portions of the inlet do not alter the air capture characteristics of the inlet". In addition to this, the flow throughout the intake must be supersonic for the engine to operate as a scramjet.

If this preferred supercritical state is seriously perturbed, the intake can unstart. It is desirable that this state is avoided at all costs because extra shocks form on the surface of the intake to allow for mass flow spillage which can increase the aerodynamic drag acting on the intake and loading on the vehicle airframe by up to a factor of 10 [2]. Furthermore, the airflow delivered to the combustor is reduced and may even be subsonic, possibly leading to flame out, and certainly reducing the total thrust

[1] *Fluid Gravity Engineering Ltd., Emsworth, United Kingdom, Corresponding author email: Andrew.hyslop@fluidgravity.co.uk*
[2] *Oxford Thermofluids Institute, University of Oxford, Oxford, United Kingdom*

generated. Heiser and Pratt [2] state that there are three types of disturbance that can cause an inlet to unstart:

1. The freestream Mach number is reduced sufficiently below the starting value.
2. The flow reaching the inlet face is sufficiently distorted so that it can no longer pass through the throat area. These distortions include total pressure losses, flow angularity, blockage, changes in angle of attack and boundary layer separation on the compression surfaces.
3. The backpressure to the intake is increased to the point that a terminal normal shock is moved upstream to the throat.

Unstart induced by raising the inlet back-pressure, e.g. from release of heat due to combustion, leads to unsteady modes of intake operation which all include mass spillage for some period. These modes of operation are generally called "buzz". Buzz is highly undesirable because the pressures within the isolator can fluctuate between very large subsonic unstart pressures to low reverse flow pressures. Buzz results in highly transient and cyclic aerodynamic loads on the intake and the delivery of off-design flow to the combustor. Lee [3] provides a review of previous work studying hypersonic inlet buzz and defines three sub-categories of buzz which are also seen by Tan [4] [5] and Wagner [6]:

- "Small amplitude oscillatory unstarted flow" (known also as small buzz). In this mode a strong oblique shock forms across the cowl entrance caused by a separation bubble. The oblique shock oscillates from an upstream position impinging on the cowl leading edge causing spillage, to a downstream position being ingested into the isolator. The internal flow is subsonic.
- "Large amplitude oscillatory unstarted flow" (also known as big buzz). In this mode the intake cycles through phases of started operation and reverse flow, with the intake shock structure drastically changing as flow is ejected upstream.
- "Non-oscillatory unstarted flow". In this mode an oblique shock forms across the cowl entrance due to a separation bubble resulting in constant spillage over the cowl.

Therefore, knowledge of how an intake operates with certain back-pressures and geometrical configurations is important for understanding the performance of the intake. It is vital that the unstarted states are avoided in flight due to the drop in performance associated with them. This paper describes the design and investigation of the self-starting behaviour and operational regimes of a three-stage mixed compression intake at a range of imposed back pressures and two isolator heights. Longer duration hypersonic wind tunnels suitable for aerodynamic experiments do not typically match the flight enthalpy, and hence the combustion processes if of interest, need to be replicated by other means. By restricting the flow at the end of the isolator, a backpressure can be imposed on the intake similar to a combustion induced pressure. Varying the restriction and therefore backpressure allows for the operational behaviour of the intake to be investigated.

2. Experimental Setup

This section describes the facility that the intake experiments were conducted in, the design and components of the intake model, the instrumentation and measurements taken during the experiments, and the optical setup used for schlieren imagery.

2.1. Facility and Freestream Conditions

The intake experiments were conducted in the University of Oxford's High Density Tunnel (HDT). This facility is a Ludwieg tube which produces high Reynolds number, cold flow suitable for aerodynamic experiments at Mach numbers between 4 and 7. A "shot" is performed by opening a fast-acting valve to allow high pressure heated gas to expand through a nozzle and flow over the model. A schematic of the facility is shown in Fig. 1 and further details about the facility and its operation can be found in McGilvray *et al.* [7].

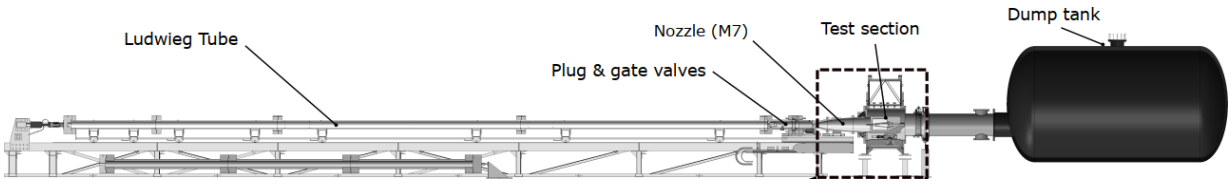

Fig 1. Schematic of the University of Oxford High Density Tunnel [8].

Prior to conducting the intake experiments, the test condition was characterised using a rake instrumented with pitot pressure probes and temperature probes. Freestream total pressure is also measured in the facility for all tests. The calculation of flow properties assumes that the test conditions are repeatable between individual shots. Mach number was calculated through the ratio of pitot-to-static pressures, viscosity using Keyes' Law [9] and all other freestream parameters were calculated through isentropic relations assuming perfect gas relations. Table 1 presents the measured and calculated freestream conditions for these experiments. The freestream conditions presented were averaged over the second plateau of the facility as shown in Fig. 2. The second plateau was selected as the total temperature and hence Reynolds number have not settled until this plateau.

For the Mach 7 condition, the size of the core flow is 280 mm at nozzle exit reducing to 240 mm at 300 mm downstream [10]. The angularity of the flow was determined to be within ± 0.12° within the core flow at this condition using Eilmer4 (a Computational Fluid Dynamics (CFD) software) [11].

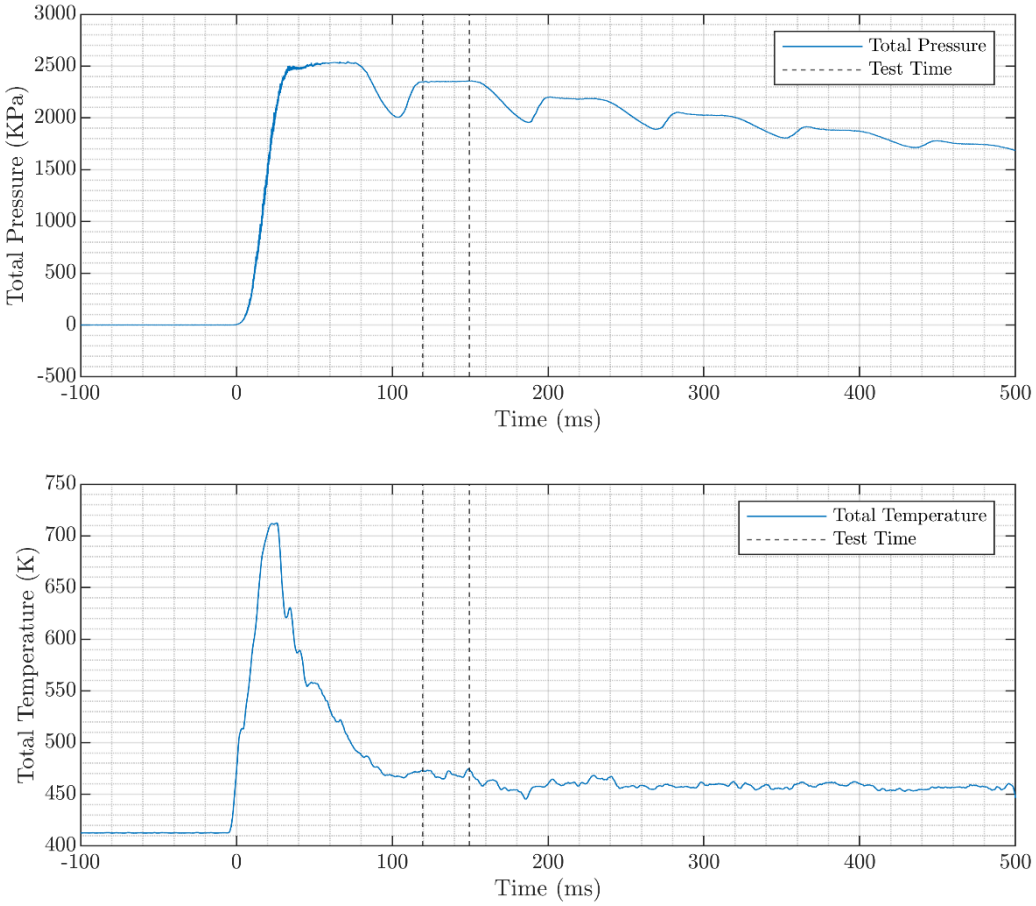

Fig 2. Freestream total pressure (top) and total temperature (bottom) with test time indicated, measured with instrumented rake prior to the intake experiments

Table 1. Test-time average flow properties.

Property	Value
Total Pressure, kPa	2357 ± 5
Pitot Pressure, kPa	37.2 ± 0.5
Total Temperature, K	468 ± 15
Mach Number	6.96 ± 0.02
Velocity, $m \cdot s^{-1}$	923 ± 12
Density, $kg \cdot m^{-3}$	0.046 ± 0.002
Static Pressure, Pa	592 ± 12
Static Temperature, K	43 ± 1.2
Dynamic Viscosity, μPa·s	3.1 ± 0.1
Dynamic Pressure, kPa	19.5 ± 0.4
Unit Reynolds Number, $\times 10^6\ m^{-1}$	13.6 ± 0.7
Reynolds Number, $\times 10^6$	4.1 ± 0.2

2.2. Intake Model

Fig. 3 shows an annotated view of the intake model with the side-plates removed to show the internal components. The intake is a three-stage 2-D mixed compression intake with an overall length of 763.5 mm, comprising of three ramps of total length 305.5 mm, an isolator of length 165 mm and a plenum with backpressure device. The intake has an overall capture area of 6.3 x 10^{-3} m^2. The intake passes the captured flow through an isolator and exhausts it into a settling plenum chamber. The backpressure within the plenum is controlled by an actuating backpressure device which can be moved to change the restriction to the flow venting out of the model, simulating pressures caused by combustion. The throttle ratio in this work is defined as follows:

$$\Delta = 1 - \frac{A_{choke}}{A_{capture}} = 1 - \frac{h_{choke}}{h_{capture}} \quad (1)$$

Where h_{choke} is the minimum distance between the actuating wedge and choke wedge and $h_{capture}$ is the vertical distance between model leading edge and the cowl leading edge. The position of the actuating wedge is measured using WayCon LZW2 potentiometer with the actuating wedge touching the choke wedge as the zero reference. The measurements from the potentiometer are recorded during experiments to confirm that the back pressure device remains stationary in the flow.

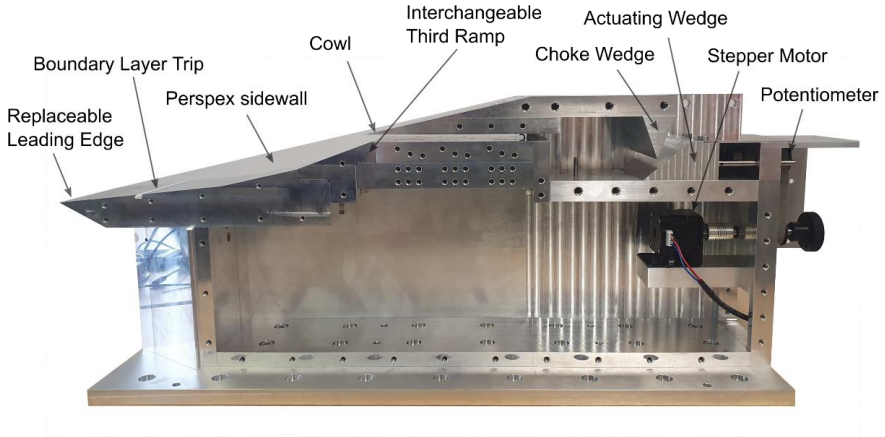

Fig 3. Annotated diagram of the intake with sidewalls removed model prior to instrumentation.

The length of the compression ramps is a 1/5 scale of the X-43a flight vehicle [12]. It is designed to operate at a Mach 7 flight representative condition and deliver a pressure of 100 kPa and temperature of 1000 K (in flight) at the end of the isolator (to a theoretical combustor). The required compression ratio to achieve this is 83.5.

A boundary layer code was used to predict the displacement thickness of the flow on the ramp surfaces, and this was removed from the inviscid surface to prevent loss in efficiency and mass capture from compressed flow being displaced. Table 2 gives the inviscid and viscous-corrected ramp angles, measured relative to the freestream flow direction.

Table 2. Intake ramp angles.

Ramp	Location, x/L	Inviscid ramp angle (°)	Viscous-corrected ramp angle (°)
1	0	5.7	5.2
2	0.52	12.4	12.1
3	0.76	20.3	20.1

Two nominal isolator heights of 5.9 mm and 7.0 mm were tested. Changing the isolator height is achieved by swapping part of the third compression ramp. This change also brings the start of the isolator slightly upstream. The smaller isolator height is closer to self-starting limits given by Kantrowitz [13], Flock [14], and Sun [15]. The self-starting behaviour of the intake as a function of variation from the nominal isolator height is investigated in Section 3. The ratio of the isolator length to duct height is designed to contain shock train including normal shock using correlations based on momentum thickness [2].

The model is designed to house interchangeable boundary layer trips, however, experiments showed that the boundary layer transitioned to turbulent before the isolator entrance with a smooth 3D printed insert. Boundary layer separation at ramp corners was avoided by considering by Korkegi correlations [16] [17]. The leading edge was also designed to be replaceable so that bluntness can be investigated if required.

Fig. 4 shows schematics of two sidewall designs that were used. The short partial sidewalls were used for all isolator heights other than the 7.0 mm height. The sidewalls are machined from Perspex to allow optical diagnostic tools to be used to visualise the flow field in the isolator of the intake if desired.

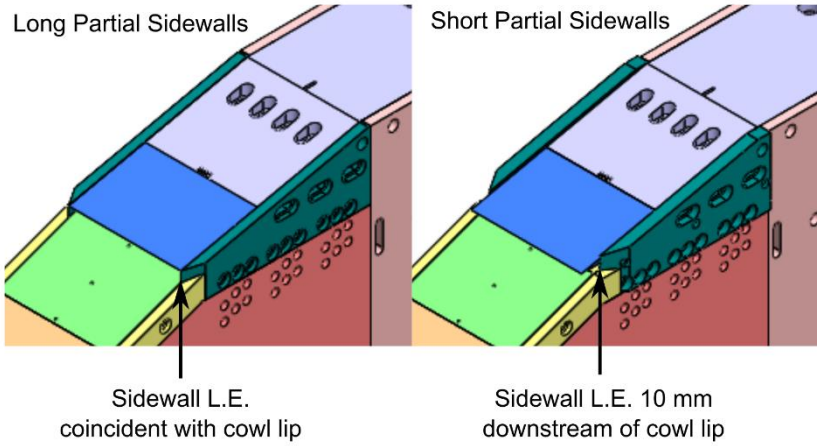

Fig 4. CAD views showing: left – long partial sidewalls that were used for isolator heights less than 7 mm, right – short partial sidewalls that were used for the 7 mm isolator height.

2.3. Instrumentation and Data Reduction

The intake model was instrumented with a high resolution of pressure transducers to maximise the characterisation of the flow field over the intake surface. Fig. 5 shows a schematic of the intake with centre-line pressure transducers and plenum thermocouples labelled. There are eight Kulite XCQ-062-10PSIA pressure transducers on the compression ramps and six Kulite XCE-062-700KPaA on the lower surface of the isolator. Not marked on the schematic are two sets of six Honeywell SSCDANN100PAAA5 transducers which are distributed along the isolator and offset by 20 mm from the centreline. These sensors provide a large coverage of the isolator surface to investigate the complex shock structure and pressure distribution in this region.

The Pitot tube instrumented with an XCEL-072-17BARA Kulite pressure transducer at the end of the isolator (140 mm from the start of the isolator) allows for the calculation of the flow local Mach number delivered to the plenum. The plenum is instrumented with a XT-190SM-17BARA Kulite and three fine gauge exposed-bead thermocouples. All transducers were sampled at 100 kHz.

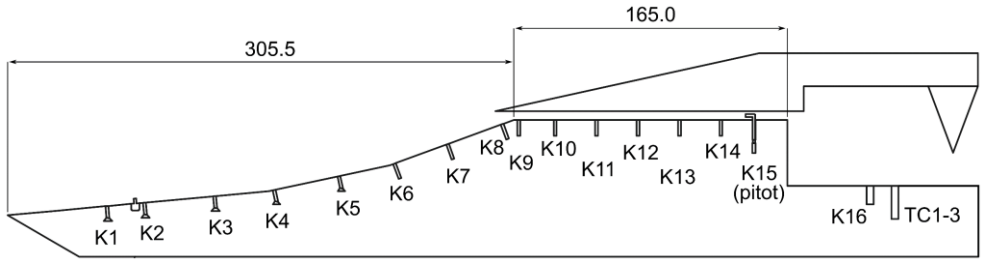

Fig 5. Scale cross-sectional schematic of the intake (5.9 mm high isolator) with centreline Kulite pressure transducer and thermocouple locations. Back pressure device not shown.

The instrumentation within the intake allowed for the following parameters to be calculated:

1. *Mach number at the end of the isolator* – Mach number is calculated using the Rayleigh-Pitot equation with the ratio of Pitot-to-static pressures of the Pitot probe (K15) to a Honeywell transducer which is 4 mm offset axially and 20 mm offset laterally.
2. *Mass flow rate* – can be calculated using flow properties in the plenum and the choke point created by the back pressure device as follows:

$$\dot{m}_{\text{plenum}} = \frac{A_{choke} p_{plenum}}{\sqrt{T_{plenum}}} \sqrt{\frac{\gamma}{R}} \left(\frac{\gamma+1}{2}\right)^{\frac{-(\gamma+1)}{2(\gamma-1)}} \quad (2)$$

Where A_{choke} is the minimum area between the wedge faces calculated from the potentiometer, p_{plenum} is the measured plenum pressure (K16), and T_{plenum} is the measured plenum temperature. This measurement assumes that the flow fully stagnates in the plenum and that measured temperature and pressure are the stagnation properties. The measurement is not expected to be highly accurate, but instead to provide a relative indication of the mass flow rate captured by the intake.

2.4. Schlieren Imagery

High speed schlieren imagery was taken using a z-type system with a Cavitar Cavalux laser as the light source and a Phantom TMX-7510 recording at a framerate of 76 kfps for the full duration of the test time. Schlieren frames presented in this work are referenced to the time that the facility is initiated rather than the start of test time. The limited size of the schlieren mirrors used means that only the third ramp and isolator entrance area was imaged. This region allows visualization of the three ramp shocks converging near the cowl and, for buzz modes, the shock train exiting the isolator entrance.

3. Self-starting Behaviour

Prior to testing the intake, the self-starting behaviour of the intake with respect to the isolator height was unknown. Multiple correlation exist in the literature which predict the self-starting behaviour based on the internal contraction ratio of the intake which is a function of isolator height [13] [15] [14]. Some correlations are more conservative than others or are created for other forms of intakes which use 3D compression. Therefore, experimental investigation is usually required to confirm that an intake is self-starting. In this investigation, the intake was tested at 5 isolator heights with a throttle of 75 %. The self-starting ability of an intake is conventionally defined relative to the internal contraction ratio of the intake:

$$\mathrm{ICR} = \frac{A_{Cl}}{A_{th}} \tag{3}$$

Where A_{Cl} is the cowl capture area and A_{th} is the throat area. Table 3 gives results of the self-starting behaviour of the intake which were investigated by incrementally increasing the height of the isolator, thereby decreasing the internal contraction ratio, and making the intake more likely to start. This was achieved by moving the cowl up within the clearance of screw holes. The intake did not start with an isolator height below 5.9 mm. Fig. 6 compares the starting behaviour against the Kantrowitz, Flock, Sun, and Isentropic starting limits as a function of ICR^{-1}. Other researchers have found the Kantrowitz limit to be conservative, yet in the current work the intake only starts once ICR^{-1} is above this limit. This shows that experimental characterisation is still required to predict if an intake is self-starting if the ICR^{-1} is reduced to that of below predicted by the Kantrowitz limit. For subsequent tests, isolator heights of greater than 5.9 mm were used.

Table 3. Self-starting behaviour.

Isolator height, mm	ICR^{-1}	Self-starting?
5.1	0.58	No
5.3	0.61	No
5.4	0.62	No
5.9	0.68	Yes
7.0	0.80	Yes

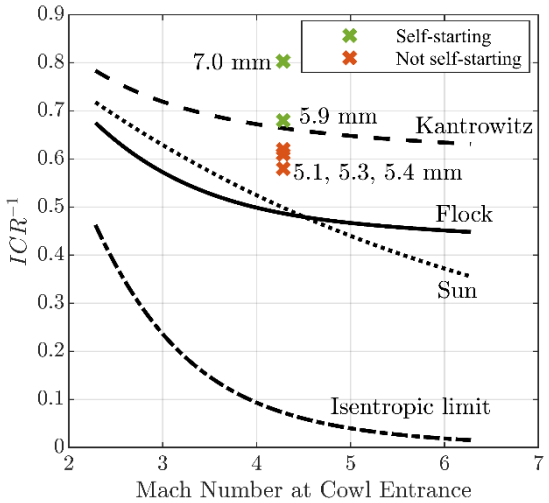

Fig 6. Self-starting behaviour of the intake compared to various self-starting criteria from the literature

4. Effect of Varying Throttle

4.1. Overview of Modes of Operation

This section discusses how the operation of the intake changes as a function of varying the throttle, and therefore as a function of backpressure. Two heights of isolator were tested: 5.9 mm and 7.0 mm. Both heights showed broadly similar behaviour as a function of throttle. Three modes of operation were identified for each height: started, started with oscillations in the isolator, and buzz. In addition, a mode of unstart without buzz was seen for the 5.9 mm isolator. Table 4 gives the values of Δ (throttle ratio) for which each of these modes was identified at.

Table 4. Operational modes

Mode	5.9 mm	7.0 mm
Started	≤ 80 %	≤ 80 %
Started with oscillations in the isolator	82.5 %	82.5 % - 85 %
Unstarted without reverse flow	85 %	Not seen
Unstarted with reverse flow (buzz)	> 85 %	≥ 87.5 %

In the following section each operational mode is described using schlieren imagery for the 5.9 mm isolator height. Equivalent schlieren was gathered for the 7.0 mm height but is not shown. Following this, measured pressures and the Mach number at the end of the isolator are used to identify key features of each mode, and to discuss the effect that each mode would have on the operation of a scramjet using this design of intake.

4.2. Details of Each Mode

Fig. 7 shows test-time average pressures normalised by the freestream static pressure with throttle ratio at three locations: a) the final transducer on the third compression ramp; b) the final transducer in the isolator; c) the pressure in the plenum (see Fig. 5 for schematic of sensor locations). Fig. 8 shows the Mach number measured at the downstream end of the isolator. Fig. 9 shows the measured mass flow rate past the choke point in the backpressure device and Fig. 10 shows the normalised pressures for all centreline pressure sensors averaged over the test time for all four modes of operation. All of these figures are referenced as each mode of operation is discussed in detail below.

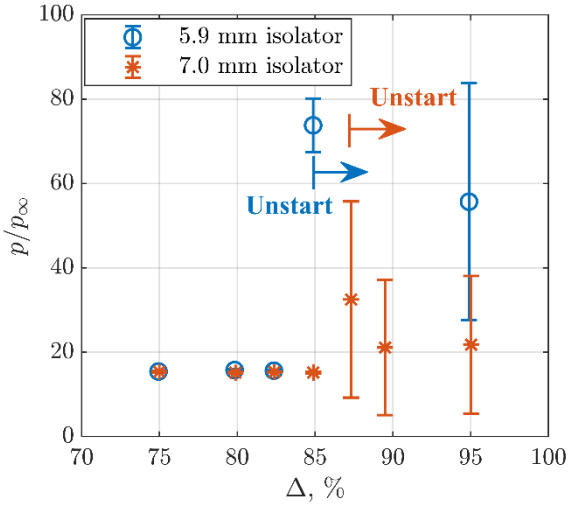

a) Most downstream transducer on the compression ramps (K8).

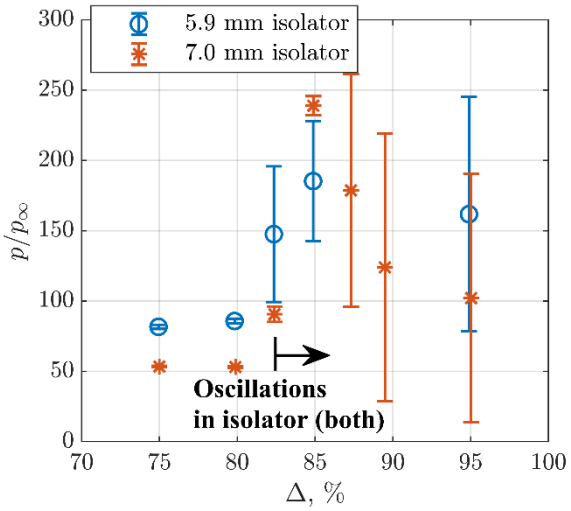

b) Most downstream transducer in isolator (K14).

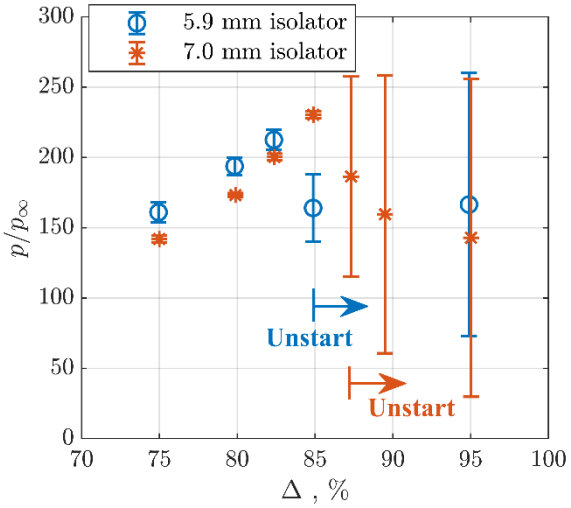

c) Plenum (K16).

Fig 7. Test-time average normalised pressures with throttle ratio. Error bars are two standard deviations.

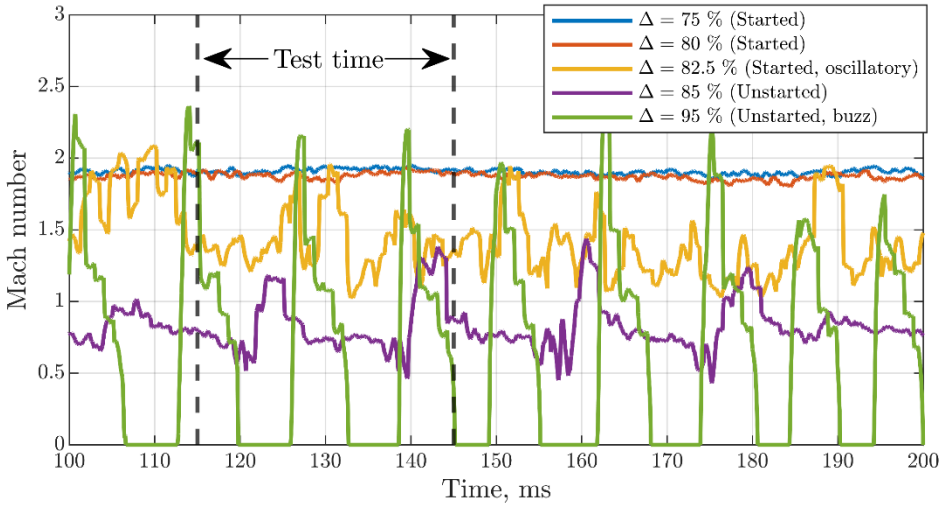

Fig 8. Mach number for the 5.9 mm isolator as a function of throttle ratio at the downstream end of the isolator (at the Pitot probe K15).

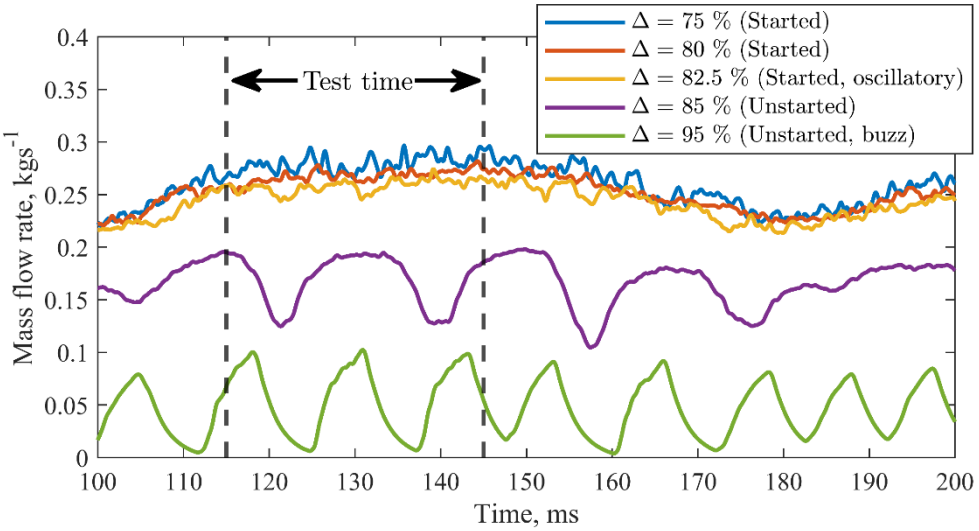

Fig 9. Mass flow rate measured past the choke in the plenum

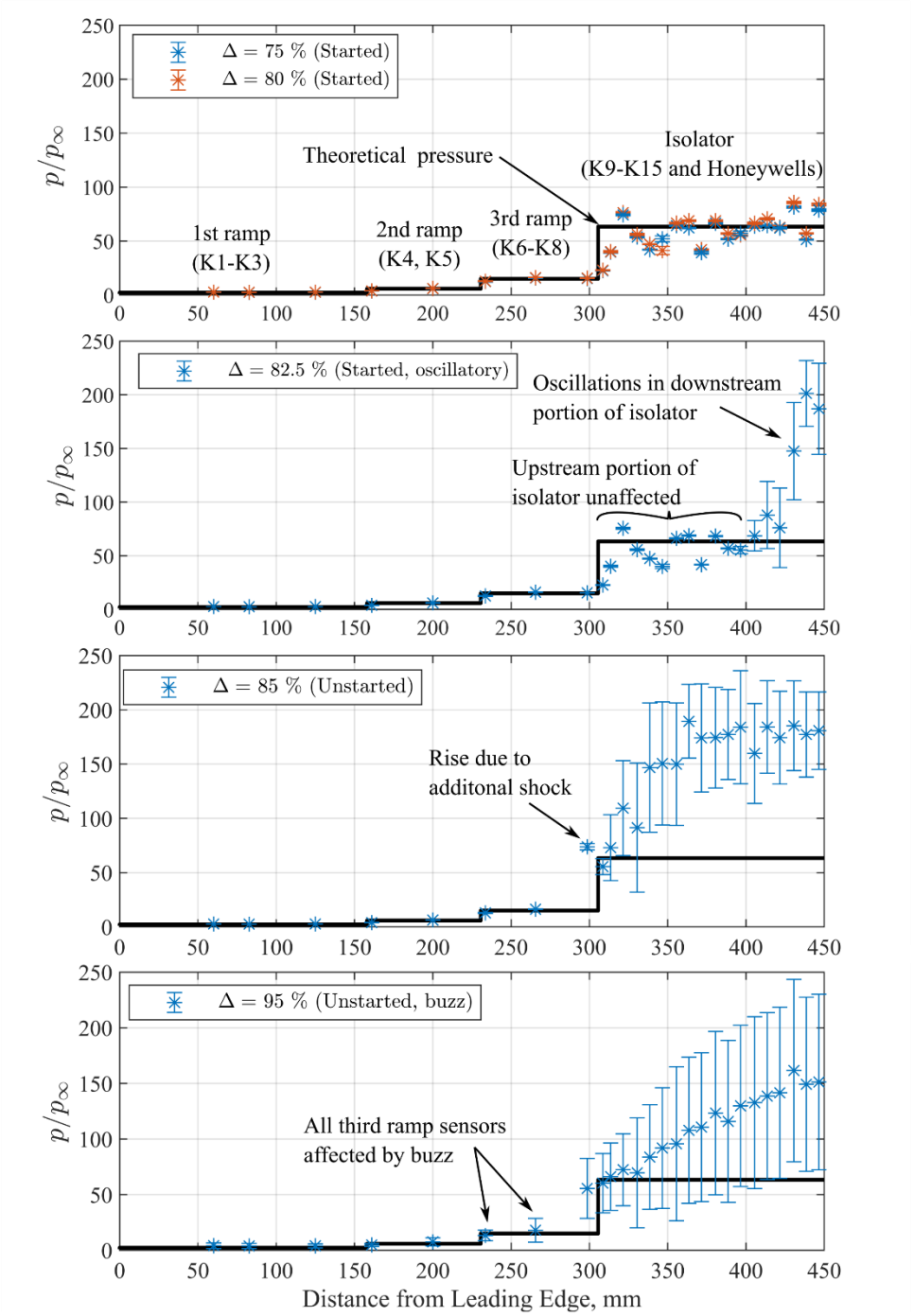

Fig 10. Normalised pressures averaged over test time across the compression ramps and isolator for all four modes of operation. Error bars are two standard deviations.

4.2.1. Started Mode

Fig. 11 shows a schlieren frame with Δ = 75 % when the intake is started. The shocks from the three compression ramps are shown to converge just above the cowl lip. Whilst all three do not intersect at a single point, they all pass upstream of the cowl so that some spillage exists, and they are not being swallowed by the isolator. The interaction of the return shock from the cowl and the expansion fan from the shoulder at the junction between the third ramp and the isolator is hidden by the chamfer on the sidewall. Shocks are reflected down the length of the isolator which can be seen to decrease in intensity as they propagate downstream.

Fig. 7 shows that the pressure on the third ramp and in the isolator are essentially unchanged up to Δ = 75 % and that the pressure recovery in the plenum increases as the throttle ratio is increased. Fig.

8 shows that the Mach number at the end of the isolator is around 1.9 and therefore the flow is supersonic until the plenum.

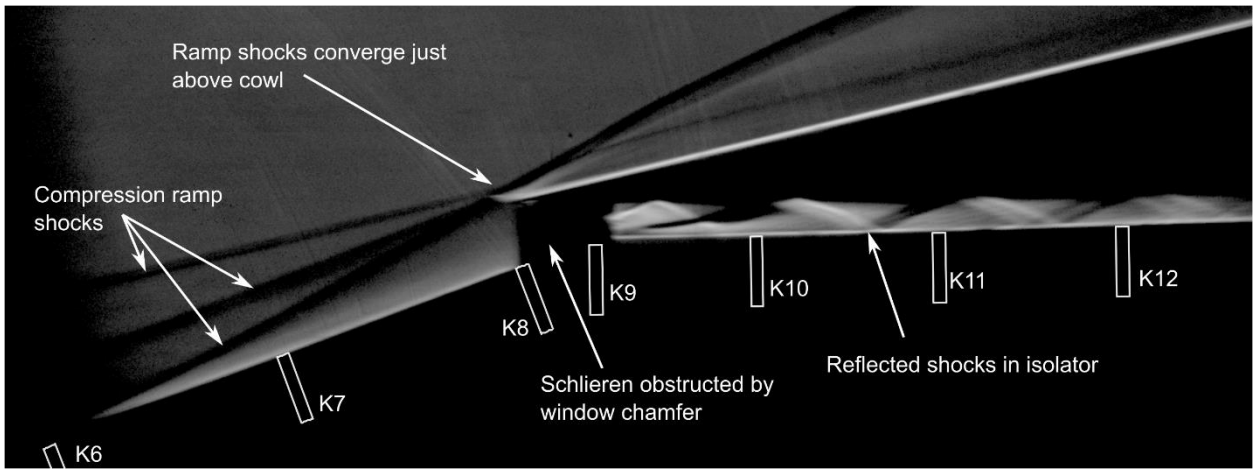

Fig 11. Schlieren image of the 5.9 mm isolator in started mode of operation with $\Delta = 75$ %.

4.2.2. Started with Oscillations in the Isolator

Fig. 12 shows a progression of schlieren images within the isolator. The cowl entrance is not in view because the field of view of the schlieren mirrors was changed to focus on the downstream end of the isolator. The tip of the pitot probe is just visible at the downstream end of the images. The images show that the shock train is oscillating by around 50 mm. This oscillation can be seen clearly in Fig. 7b) as the large standard deviation in measured static pressure at the end of the isolator. Fig. 9 shows that the mass capture in this mode of operation is the same as the started case and therefore the intake is still considered to be started. Despite this, the conditions delivered to the end of the isolator are highly off-design and in a real scramjet would have a detrimental effect on combustion. Additionally, the pressure recovery in the isolator is lower than the started mode.

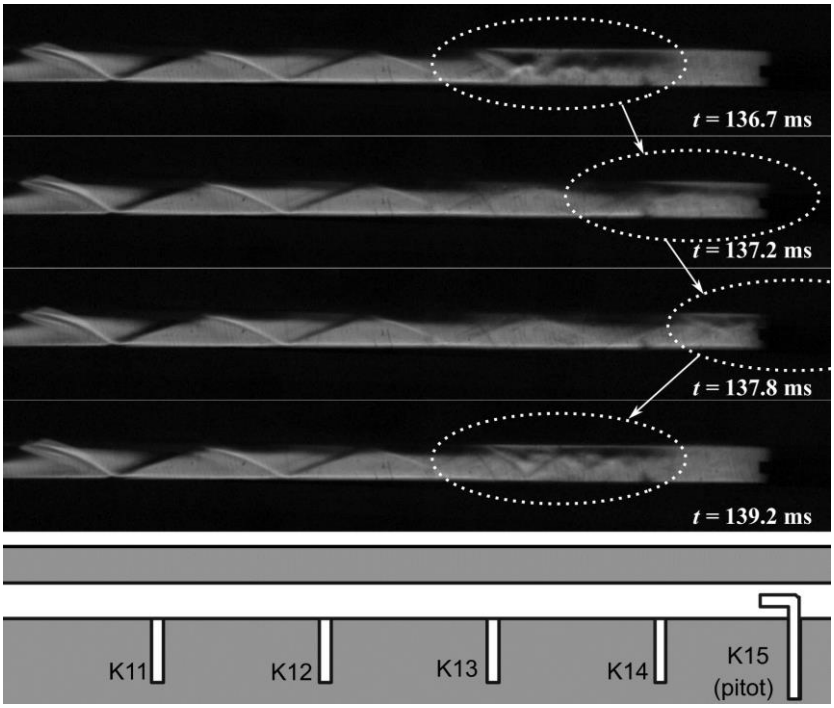

Fig 12. Schlieren images of oscillations in the isolator for $\Delta = 82.5$ % with the 5.9 mm isolator height. Schematic is shown to locate field of view on the model.

4.2.3. Unstarted without Buzz

This mode of operation was seen at $\Delta = 85$ % for the 5.9 mm isolator but never seen for the 7.0 mm isolator. A schlieren image of the unstarted intake can be seen in Fig. 13. At this throttle the intake is unstarted: internal flow structures have resulted in an additional shock forming across the isolator entrance which spills additional mass above the cowl. The effect of unstart is clearly seen on all measurements:

- Fig. 7 shows that the additional shock results in a rise in pressure on the third ramp, increased static pressure at the end of the isolator, and a reduction in pressure recovery in the plenum.
- Fig. 8 shows that the flow delivered to a combustor at the end of the isolator is mostly subsonic: an engine would not be operating as a scramjet in this mode.
- Fig. 9 shows a reduction in mass capture of around a third compared to the started level. This would lead to a reduction in net thrust.

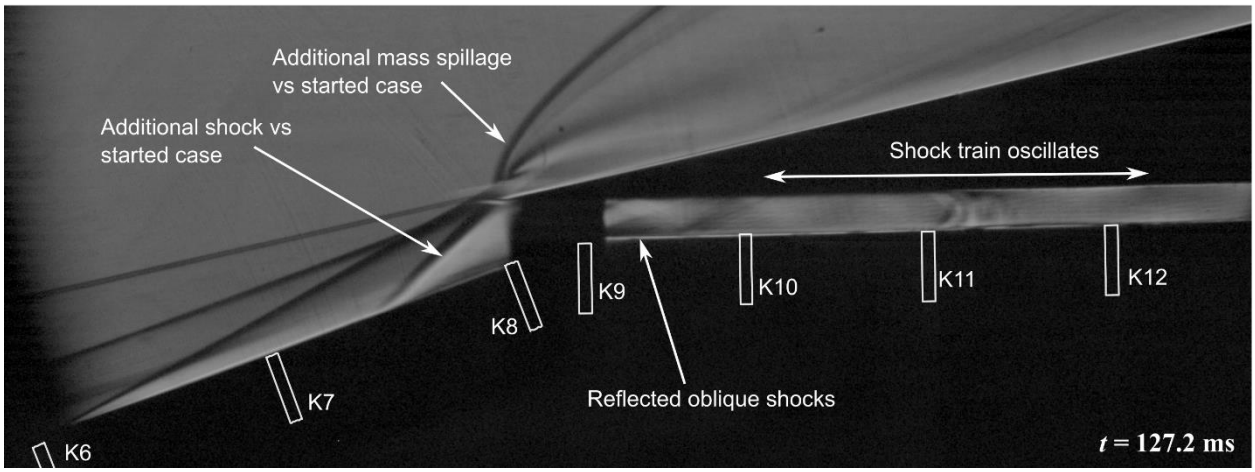

Fig 13. Schlieren image of the intake with $\Delta = 85$ %.

4.2.4. Unstarted with Buzz

When the backpressure is increased to 95 % the intake enters a state referred to as buzz. The buzz seen falls into the category of 'big buzz' [4] or 'large amplitude oscillatory unstarted flow' [3] in the literature. The key feature of this type of buzz is that the intake violently oscillates from being started to ejecting flow upstream from the isolator (reverse flow), drastically altering the ramp shock structures.

Fig. 14 shows a progression of schlieren images, starting from the intake in an unstarted state much like that seen for $\Delta = 85$ % with an additional shock across the cowl entrance. The shock train then moves upstream within the isolator, eventually resulting in reverse flow with a bow shock in front of the intake. Eventually the flow direction reverses again, the shock structure collapses back down, and the intake returns to the starting state. Again, the effects of buzz can be seen in the measurements:

- Fig. 7 shows large oscillations at each measurement location along with an even greater reduction in average pressure recovery in the plenum.
- Fig. 8 shows that the flow is temporarily supersonic once each cycle which happens immediately after the flow changes direction to match the freestream, and the plenum is at its lowest pressure in the cycle. Fig. 8 also shows that the frequency of the buzz cycle is around 45 Hz. The frequency is dependent on the isolator and plenum filling and emptying, and is therefore a function of the volume of these regions.
- The mass flow rate measurement in Fig. 9 is not valid because the flow is not always choked at the wedge for this mode. However, taking the measurement as a proxy for plenum pressure, it shows qualitatively how the buzz is dictated by emptying and filling of the plenum volume, with the pressure slowly responding to the change in flow structure and direction.

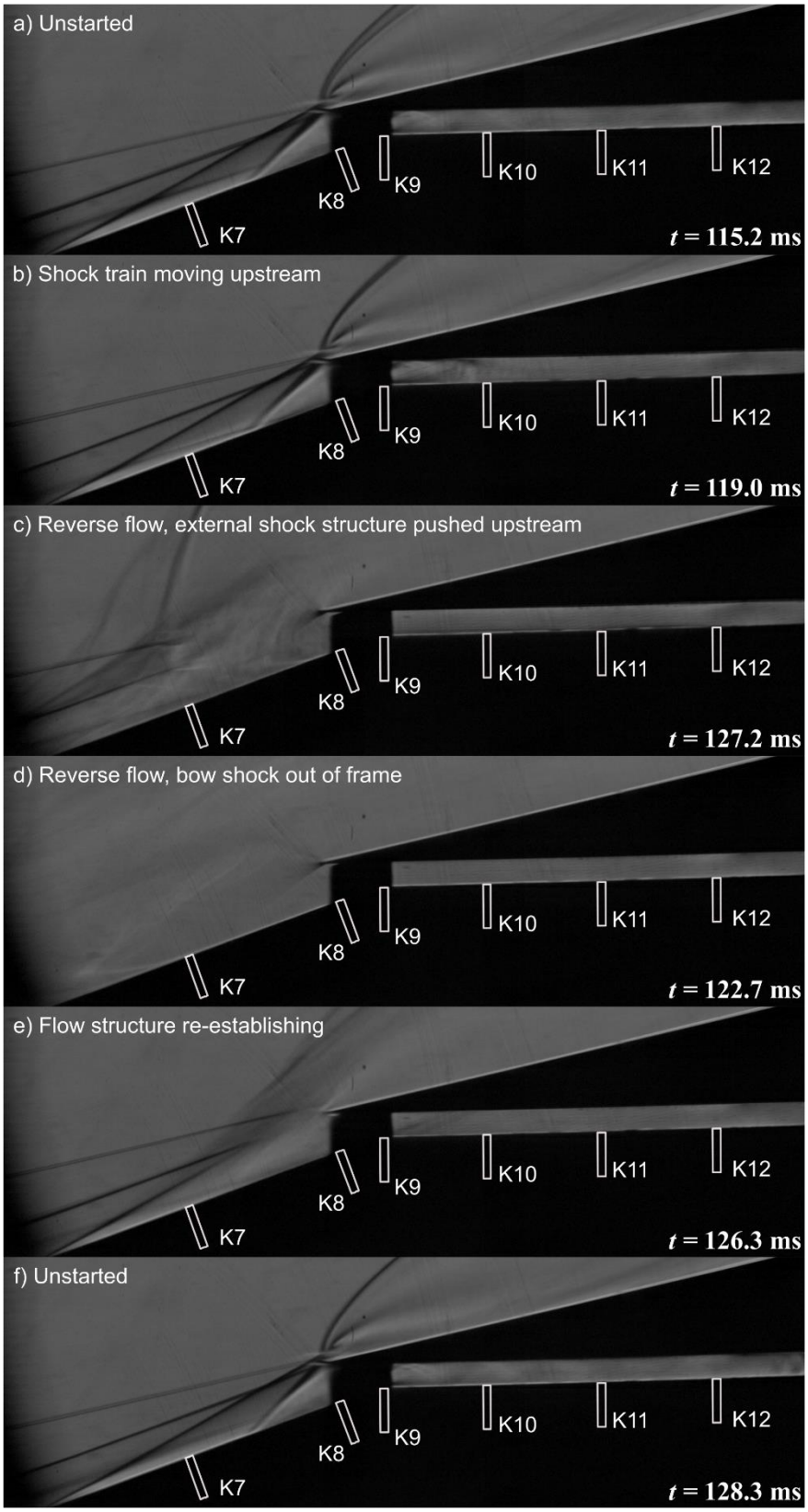

Fig 14. Schlieren images with $\Delta = 95$ % showing a buzz cycle.

5. Conclusions

A newly designed mixed compression intake has been calibrated in the University of Oxford High Density tunnel. The intake configuration is shown to be highly sensitive to back-pressure and isolator height. The self-starting ability of the intake with isolator heights below the Kantrowitz limit were shown to be not self-starting for this intake configuration, showing the need to be conservative when using other self-starting empirical relations in the literature. With the isolator height at 5.9 mm, four different operating regimes were identified based on the applied backpressure to the isolator. The experiments successfully showed that an intake behaviour can be characterised with varying back-pressure and this approach can be extended to more complex intakes in the future.

References

[1] D. M. Van Wie, E. T. Curran and S. N. B. Murthy, "Scramjet propulsion," *American Institute of Aeronautics and Astronautics. Chap. Scramjet Inlets,* p. 447, 2000.

[2] W. H. Heiser and D. T. Pratt, Hypersonic airbreathing propulsion, AIAA, 1994.

[3] J. Lee, S. G. Lee, S. H. Kang and H.-J. Namkoung, "Numerical Study on the Non-Oscillatory Unstarted Flow in a Scramjet Inlet-Isolator Model," *Aerospace,* vol. 9, p. 162, 2022.

[4] H.-J. Tan, S. Sun and Z.-L. Yin, "Oscillatory flows of rectangular hypersonic inlet unstart caused by downstream mass-flow choking," *Journal of Propulsion and Power,* vol. 25, p. 138–147, 2009.

[5] H.-j. Tan and e. al., "Experimental investigation of the unstart process of a generic hypersonic inlet," *AIAA journal,* vol. 49, no. 2, pp. 279-288, 2011.

[6] J. L. Wagner, K. B. Yuceil, A. Valdivia, N. T. Clemens and D. S. Dolling, "Experimental investigation of unstart in an inlet/isolator model in Mach 5 flow," *AIAA journal,* vol. 47, p. 1528–1542, 2009.

[7] M. McGilvray, L. J. Doherty, A. J. Neely, R. Pearce and P. Ireland, "The oxford high density tunnel," 2015.

[8] S. Wylie, "Hypersonic boundary layer instability measurements at low and high angles of attack," University of Oxford, 2020.

[9] F. G. Keyes, "A summary of viscosity and heat-conduction data for He, A, H2, O2, N2, CO, CO2, H2O, and air," *Transactions of the American Society of Mechanical Engineers,* vol. 73, p. 589–595, 1951.

[10] A. M. Hyslop, M. McGilvray and L. J. Doherty, "Free-flight aerodynamic testing of a 7 degree half-angle cone," 2022.

[11] P. A. Jacobs and R. J. Gollan, "The user's guide to the Eilmer4 flow simulation program," 2017.

[12] C. Bahm, E. Baumann, J. Martin, D. Bose, R. Beck and B. Strovers, "The X-43A Hyper-X Mach 7 flight 2 guidance, navigation, and control overview and flight test results," 2005.

[13] A. Kantrowitz, Preliminary investigation of supersonic diffusers, National Advisory Committee for Aeronautics, 1945.

[14] A. K. Flock and A. Gülhan, "Modified Kantrowitz starting criteria for mixed compression supersonic intakes," *AIAA journal,* vol. 57, p. 2011–2016, 2019.

[15] B. Sun and K.-y. Zhang, "Empirical equation for self-starting limit of supersonic inlets," *Journal of Propulsion and Power,* vol. 26, p. 874–875, 2010.

[16] R. H. Korkegi, "A lower bound for three-dimensional turbulent separation in supersonic flow," *AIAA journal,* vol. 23, p. 475–476, 1985.

[17] R. H. Korkegi, "Comparison of shock-induced two-and three-dimensional incipient turbulent separation," *AIAA journal,* vol. 13, p. 534–535, 1975.